Supplemental Material for:

A Novel Polyoxometalate-based Metal-Organic Nanotube Frameworks Templated by Twin-Dawson clusters: Synthesis, Structure and Bifunctional Electrocatalytic Properties†

Borong Lu, Shaobin Li*, Xiaozhou Zhang, Deqing Zhang, Linlin Fan, Eryun Yan*, Yongjuan Zhang and Liang Yu

Table of contents:

powder X-ray diffraction patterns for **1**.

14. **Fig. S11.** TG curve of **1**.

15. **Fig. S12.** N_2 adsorption-desorption isotherm curve of **1**.

16. **Fig. S13.** Reduction of ClO_3^- (a) and H_2O_2 (b) at **1**-GCE in 1 M H_2SO_4 solution.

17. **Fig. S14.** Reduction of BrO_3^- (a) at $(NBu_4)_6[P_2W_{18}O_{62}]$-GCE in 1 M H_2SO_4 solution and oxidation of AA (b) at $(NBu_4)_6[P_2W_{18}O_{62}]$-GCE in N_2 purged solution.

18. **Fig. S15.** The 100 consecutive CV cycles of the **1**-GCE at the scan rate of 0.1 $V \cdot s^{-1}$.

Table S1. Summarization of known POM-based coordination compounds assembled from double polyoxoanions as templates.

	Compounds	References
1	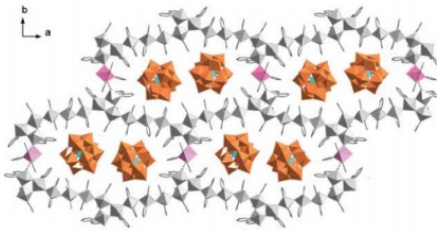 $[\{Mn(bpy)(py)(H_2O)_2\}\{Mo_{12}O_{34}(bpy)_{12}\}]$ $[PMo_{12}O_{40}]_2 \cdot 2H_2O$	*Enbo Wang et al.,* ***Chem. Commun.*** 2007, 770

2	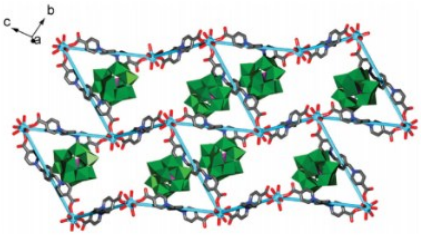 $[Ln(L)_{1.5}(H_2O)_5][PMo_{12}O_{40}]\cdot 1.5CH_3CN\cdot 2H_2O$	*Enbo Wang et al.,* ***Dalton Trans.*** 2011, 40, 5971
3	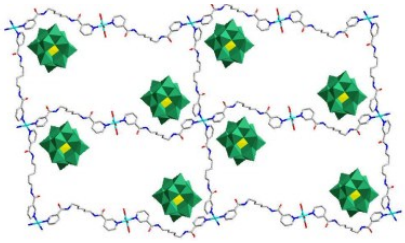 $[Cu_2(L_3)_3(SiMo_{12}O_{40})(H_2O)_6]\cdot 4H_2O$ $[Cu_2(L_3)_3(SiW_{12}O_{40})(H_2O)_6]\cdot 4H_2O$	*Xiuli Wang et al.,* ***CrystEngComm***. 2012, 14, 5836
4	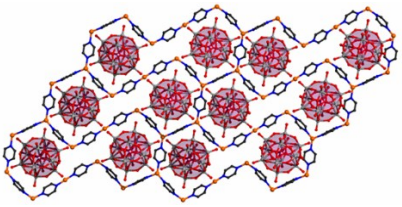 $[Cu_5(pz)_6(H_2O)_4][PW^{VI}_{10}W^{V}_{2}O_{40}]$	*Shaobin Li et al.,* ***New Journal of Chemistry*** 2014, 38, 4963
5	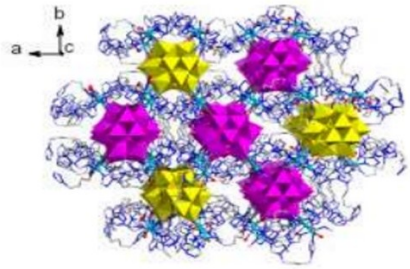 $H_2[Cu_{11}(btb)_{19}(H_2O)_6(P_2W_{16}{}^{VI}W_2{}^{V}O_{62})_3]$ $\cdot 12H_2O$	*Shaobin Li et al.,* ***Dalton Trans.*** 2015, 44, 2062

6	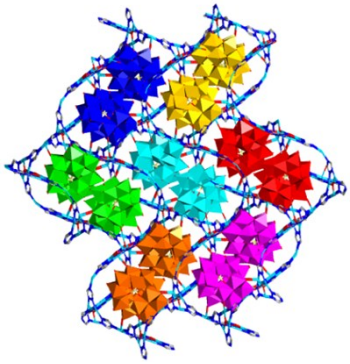 [{$Cu_3(\mu_3$-O)}$_2$(trz)$_6$$Cu_2$($H_2O$)$_{13}$][$H_{1.73}P_2As_{1.73}W_{16.27}O_{62}$]·8.25$H_2O$	This work

Table S2. The selected bond lengths (Å) and angles (º) for compound **1**.

Compound 1			
W(1)-O(1)	1.694(12)	W(1)-O(6)	1.928(11)
W(1)-O(2)	1.912(14)	W(1)-O(7)	1.878(14)
W(2)-O(2)	1.914(7)	W(2)-O(4)	1.916(8)
W(2)-O(3)	1.660(10)	W(2)-O(8)	1.886(10)
O(16)-P(2)	1.538(10)	P(1)-O(56)	1.588(13)
Cu(1)-N(8)	2.009(14)	Cu(1)-O(63)	1.960(12)
Cu(2)-N(12)	1.946(14)	Cu(2)-O(63)	1.999(11)
Cu(3)-N(9)	1.961(12)	Cu(3)-O(63)	2.058(11)
Cu(4)-N(4)	1.951(15)	Cu(4)-O(64)	2.012(10)
Cu(5)-N(5)	1.983(13)	Cu(5)-O(64)	1.899(15)
Cu(6)-N(7)	1.960(12)	Cu(6)-O(64)	1.999(11)
Cu(7)-N(17)	1.911(10)	Cu(7)-O(38)	2.278(14)
O(1)-W(1)-O(2)	97.74(6)	O(2)-W(1)-O(16)	75.41(8)
O(16)-W(1)-O(7)	83.86(8)	O(2)-W(2)-O(16)	73.56(8)
O(3)-W(2)-O(10)	101.56(6)	O(2)-W(2)-O(3)	100.51(5)
N(14)-Cu(1)-O(63)	87.31(5)	P(1)-O(42)-W(12)	128.34(6)
N(8)-Cu(1)-N(14)	178.63(5)	P(2)-O(11)-W(9)	128.13(5)
N(9)-Cu(3)-O(63)	92.30(6)	N(12)-Cu(2)-O(63)	88.88(7)
N(9)-Cu(3)-N(11)	177.39(7)	N(12)-Cu(2)-N(13)	170.70(5)
N(1)-Cu(4)-O(64)	86.81(4)	N(5)-Cu(5)-O(64)	89.89(6)
N(1)-Cu(4)-N(4)	174.20(7)	N(5)-Cu(5)-N(6)	173.20(7)

N(2)-Cu(6)-O(64)	87.01(6)	N(18)-Cu(7)-O(38)	109.27(6)
N(2)-Cu(6)-N(7)	163.33(7)	N(18)-Cu(7)-N(17)	95.24(7)

Symmetry transformations used to generate equivalent atoms: #1 1-x,1-y,1-z.

Table S3 Comparison of electrochemical between the present compound **1** and POM based hybrids on oxidation of AA.

Material	**Concentration of AA**	**electrocatalytic efficiency**	**Electrolyte Refs**
$Cu_5(pzta)_6(H_2O)_2[Mo_8O_{26}]$	0.3mM	77.8%	1M H_2SO_4 [1]
$\{[Co(L)_4][HPMo_8V^V_4O_{40}(V^{IV}O)_2]\}$	0.8mM	43%	0.5M H_2SO_4 [2]
$[Cu(Pz)](V_4O_{10})$	6 mM	208.3%	1M H_2SO_4 [3]
$(Hbib)_2[Cu(bib)(PMo_{12}O_{40})]\cdot 2H_2O$	0.4 mM	134 %	1M H_2SO_4 [4]
$[\{Cu_3(\mu_3\text{-}O)\}_2(trz)_6Cu_2(H_2O)_{13}][H_{1.73}P_2As_{1.73}W_{16.27}O_{62}]\cdot 8.25H_2O$	0.5mM	896.8 %	1M H_2SO_4 This work

References

1. S.B. Li, H.Y. Ma, H.J. Pang, Z.F. Zhang, Y. Yu, H. Liu and T.T. Yu, *CrystEngComm.,* 2014, 16, 2045-2055.

2. Y. Yu, H.Y. Ma, H.J. Pang, S.B. Li, T.T. Yu, H. Liu, C. Y. Zhao and Z.F. Zhang, *New J. Chem.,* 2014, 38, 1271-1276.

3. S. B. Li, L. Zhang, B. R. Lu, E. Y. Yan, T. H. Wang, L. Li, J. X. Wang, Y. Yu and Q. D. Mu, *New J. Chem.,* 2018, 42, 7247−7253.

4. B.R. Lu, Y.C. Wu, S.B. Li, X.Y. Yang, E.Y. Yan, J. Chen, H.W. Ma, J. Wang, Y.X. Zhu and D.W.Tao, *J Coord Chem.,* 2019, 72, 283-293.

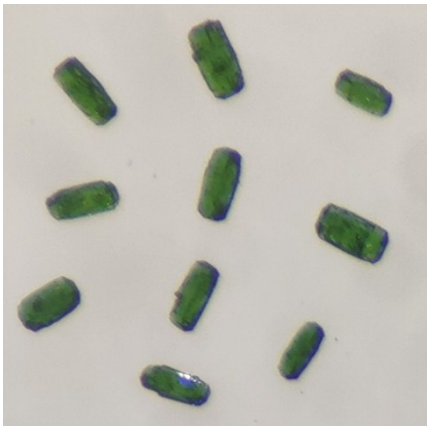

Fig. S1. The images of compound **1** under an optical microscope**.**

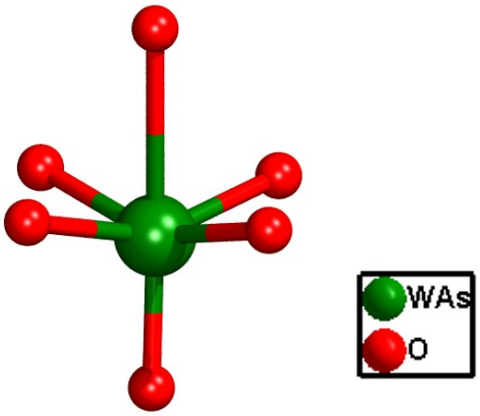

Fig. S2. The W/As with isomorphously substituted sites exhibit octahedral coordination modes.

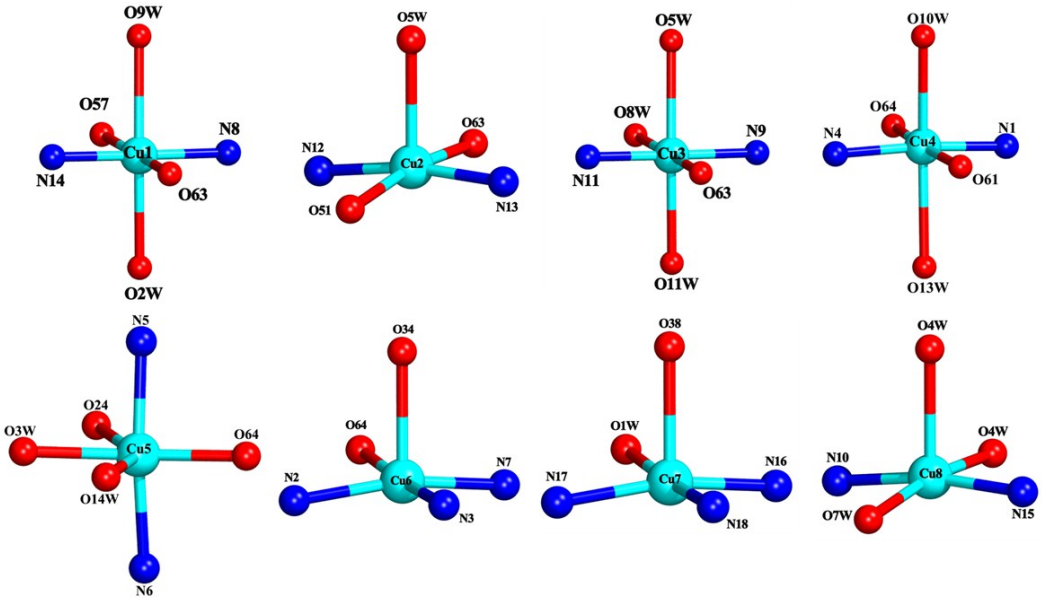

Fig. S3. The eight crystallographically independent Cu ions in **1**.

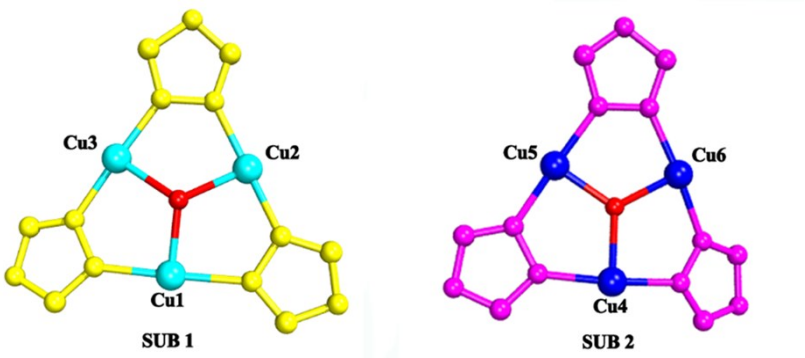

Fig. S4. The SBU1 and SBU2.

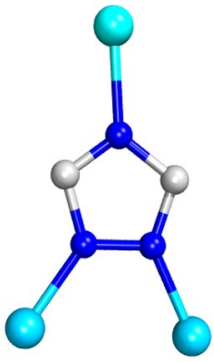

Fig. S5. The trz ligands adopt μ_3 coordination mode to link with three Cu cations.

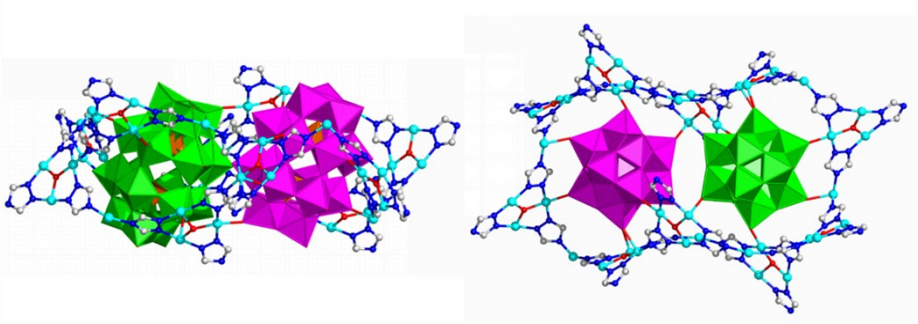

Fig. S6. The twin-Dawson clusters as templates are encapsulated by $Cu_{38}(trz)_{30}$ macrocycl window.

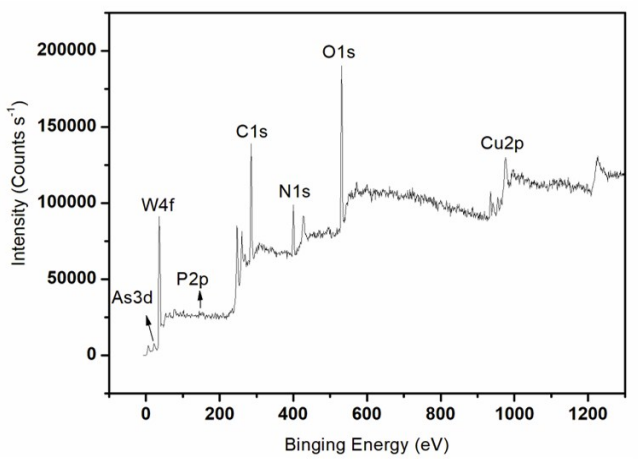

Fig. S7. The XPS spectrum of **1**.

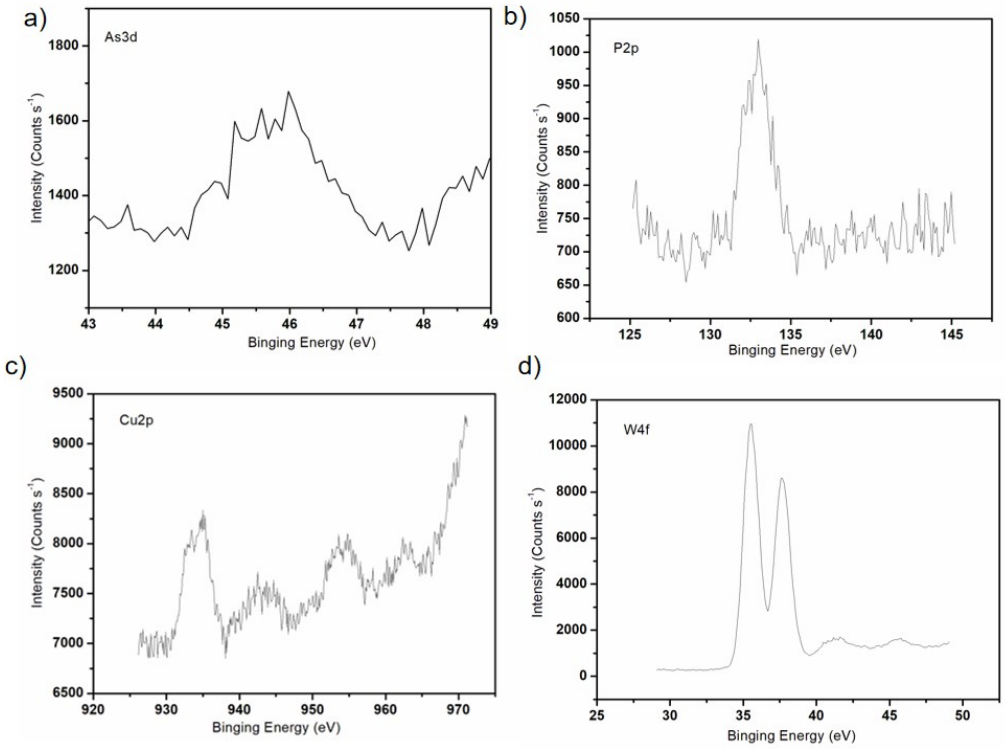

Fig. S8. The XPS high-resolution As3d, P2p, Cu2p and W4f peaks in **1**.

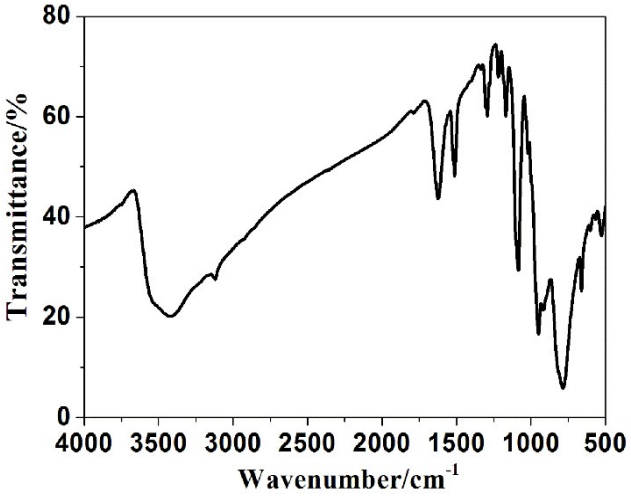

Fig. S9. The IR spectrum of **1**.

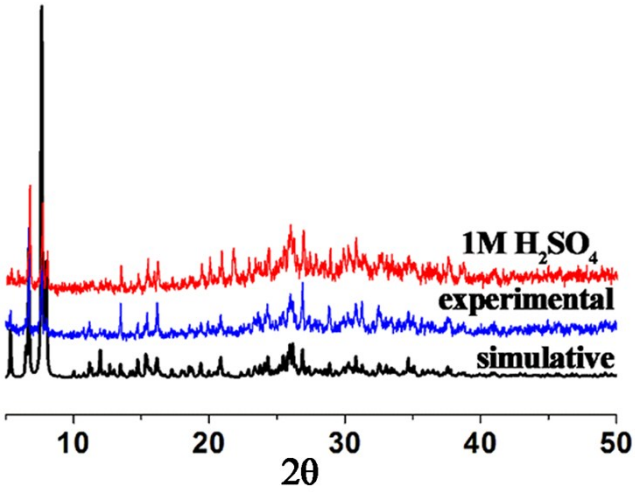

Fig. S10. The simulative (black), experimental (blue) and soaked in 1M H_2SO_4 (red) powder X-ray diffraction patterns for **1**.

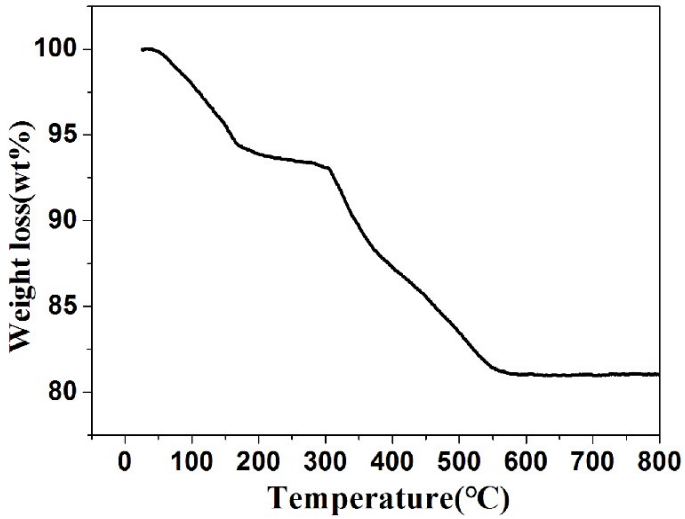

Fig. S11. TG curve of **1**.

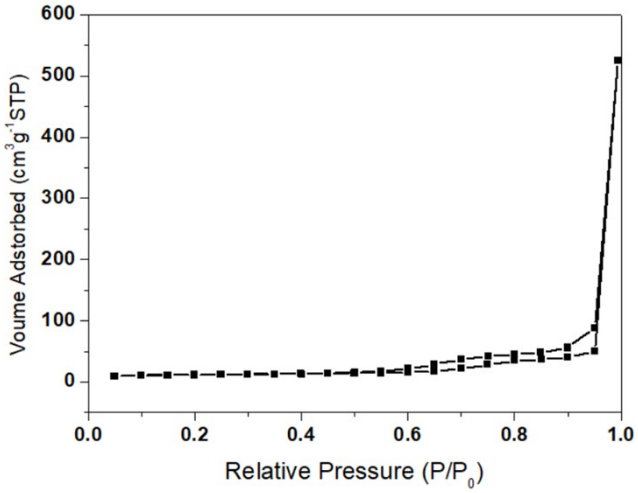

Fig. S12. N_2 adsorption-desorption isotherm curve of **1**.

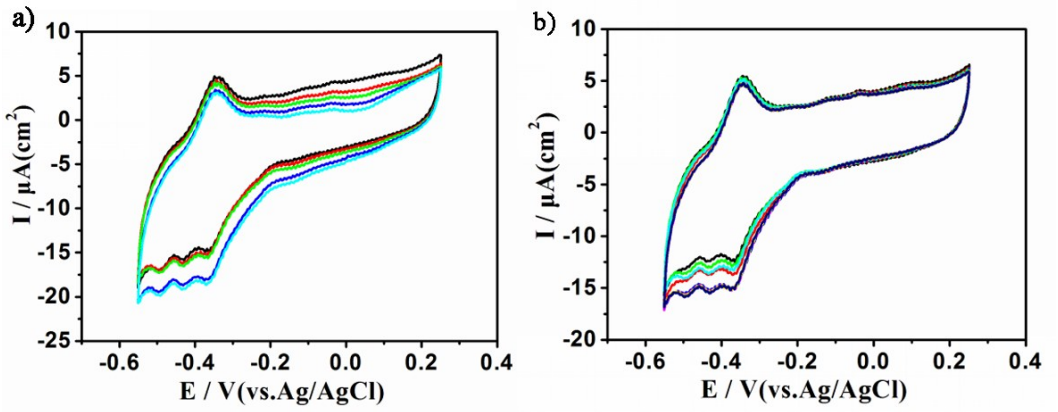

Fig. S13. Reduction of ClO_3^- (a) and H_2O_2 (b) at **1**-GCE in 1 M H_2SO_4 solution (scan rate: 0.1 V·s^{-1}) containing ClO_3^- and H_2O_2 in various concentrations: 0, 0.1, 0.2, 0.3, 0.4, 0.5 mM.

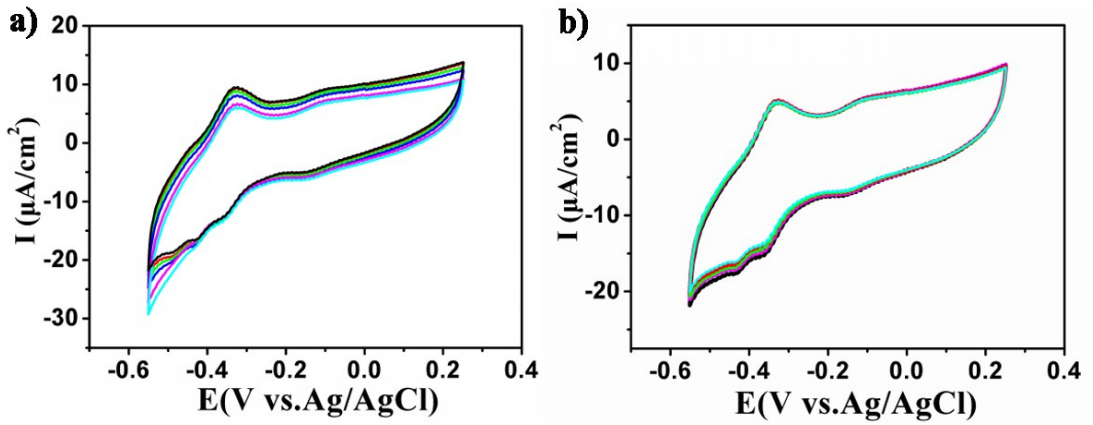

Fig. S14. Reduction of BrO_3^- (a) at $(NBu_4)_6[P_2W_{18}O_{62}]$-GCE in 1 M H_2SO_4 solution and oxidation of AA (b) at $(NBu_4)_6[P_2W_{18}O_{62}]$-GCE in N_2 purged solution (scan rate: 0.1 $V \cdot s^{-1}$) containing BrO_3^- and AA in various concentrations (from top to bottom): 0, 0.1, 0.2, 0.3, 0.4, 0.5 mM.

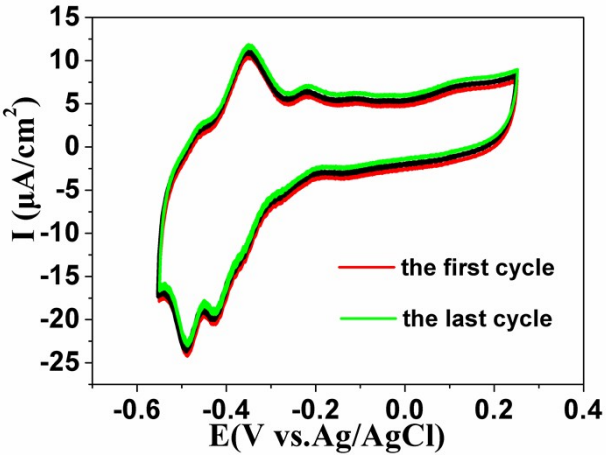

Fig. S15. The 100 consecutive CV cycles of the **1**-GCE at the scan rate of 0.1 $V \cdot s^{-1}$ in 1 M H_2SO_4 solution.